

Improved focusing with Hypergeometric-Gaussian type-II optical modes

Ebrahim Karimi^{1,2,*}, Bruno Piccirillo,¹ Lorenzo Marrucci,^{1,2} and
Enrico Santamato^{1,*}

¹*Dipartimento di Scienze Fisiche, Università degli Studi di Napoli “Federico II”, Complesso
di Monte S. Angelo, 80126 via Cintia Napoli, Italy*

²*Consiglio Nazionale delle Ricerche-INFN Coherentia, Università di Napoli, Italy*

**Corresponding authors: karimi@na.infn.it, enrico.santamato@na.infn.it*

Abstract: We present a novel family of paraxial optical beams having a confluent hypergeometric transverse profile, which we name hypergeometric Gauss modes of type-II (HyGG-II). These modes are eigenmodes of the photon orbital angular momentum and they have the lowest beam divergence at waist of HyGG-II among all known finite power families of paraxial modes. We propose to exploit this feature of HyGG-II modes for generating, after suitable focusing, a “light needle” having record properties in terms of size and aspect ratio, possibly useful for near-field optics applications.

© 2018 Optical Society of America

OCIS codes: (050.1960) Diffraction theory; (260.6042) Singular optics.

References and links

1. K. Dholakia, “Optics: Against the spread of the light,” *Nature* **45**, 413 (2008).
2. H. Wang, L. Shi, B. Lukyanchuk, C. Sheppard and C. T. Chong, “Creation of a needle of longitudinally polarized light in vacuum using binary optics,” *Nat. Photon.* **2**, 501-505 (2008).
3. G. Molina-Terriza, J. P. Torres, and L. Torner, “Twisted photons,” *Nat. Phys.* **3**, 305-310 (2007).
4. G. D. M. Jeffries, J. S. Edgar, Y. Zhao, J. P. Shelby, C. Fong, and D. T. Chiu, “Using polarization-shaped optical vortex traps for single-cell nanosurgery,” *Nano. Lett. Proc. R. Soc. London Ser. A* **7**, 415-420 (2007).
5. H. He, N. R. Heckenberg, and H. Rubinsztein-Dunlop, “Optical particle trapping with high order doughnut beams produced using high efficiency computer generated holograms” *J. Mod. Opt.* **42**, 217-223 (1995).
6. J. Durnin, J. J. M. Jr., and J. H. Eberly, “Diffraction-free beams,” *Phys. Rev. Lett.* **58**, 1499-1501 (1987).
7. J. Durnin, “Exact solutions for nondiffracting beams. I. The scalar theory,” *J. Opt. Soc. Am. A* **4**, 651-654 (1987).
8. Y. Zhao, J. S. Edgar, G. D. M. Jeffries, D. McGloin, and D. T. Chiu, “Spin-to-orbital angular momentum conversion in a strongly focused optical beam,” *Phys. Rev. Lett.* **99**, 073901 (2007).
9. J. A. Davis, D. E. McNamara, D. M. Cottrell, and J. Campos, “Image processing with the radial Hilbert transform: theory and experiments” *Opt. Lett.* **25**, 99-101 (2000).
10. J. Salo, J. Fagerholm, A. T. Friberg, and M. M. Salomaa, “Nondiffracting bulk-acoustic X waves in crystals,” *Phys. Rev. Lett.* **83**, 1171 (1999).
11. B. Richards, and E. Wolf, “Electromagnetic diffraction in optical systems II. Structure of the image field in an aplanatic system,” *Proc. R. Soc. London A* **253**, 358-379 (1959).
12. K. S. Youngworth, T. G. Brown, “Focusing of high numerical aperture cylindrical vector beams,” *Opt. Exp.* **7**, 77-87 (2000).
13. R. Dorn, S. Quabis, and G. Leuchs, “Sharper focus for a radially polarized light beam,” *Phys. Rev. Lett.* **91**, 233901 (2003).
14. Q. Zhan, “Properties of circularly polarized vortex beams,” *Opt. Lett.* **31**, 867-869 (2006).
15. M. A. Bandres and J. C. Gutiérrez-Vega, “Circular beams,” *Opt. Lett.* **33**, 177-179 (2008).
16. V. V. Kotlyar, R. V. Skidanov, S. N. Khonina, and V. A. Soifer, “Hypergeometric modes,” *Opt. Lett.* **32**, 742-744 (2007).

17. E. Karimi, G. Zito, B. Piccirillo, L. Marrucci, and E. Santamato, "Hypergeometric-Gaussian modes," *Opt. Lett.* **32**, 3053-3055 (2007).
18. H. Wang, L. Shi, G. Yuan, X. S. Miao, W. Tan and T. Chong, "Subwavelength and super-resolution nondiffraction beam," *Appl. Phys. Lett.* **89**, 171102 (2006).
-

1. Introduction

In recent years, an increasing research effort has been put into creating paraxial light beams having uncommon properties tailored for particular uses. Notable examples include non-diffracting beams [1], beams with large longitudinal non-propagating component of the field [2], and beams possessing an integer value of the photon orbital angular momentum [3]. Such special beams have found a wide range of applications, such as optical lithography, data storage, microscopy, material processing, optical trapping, optical tweezers and metrology [4, 5, 6, 7, 8, 9, 10].

Richard and Wolf [11] have shown, by using a vector Debye integral, that a non-propagating component of the electric field can be created near the focal point of high numerical aperture lens. It has been found, both theoretically [12] and experimentally [13], that a radially polarized light beam can be focused into a much tighter and deeper spot than a linearly polarized beam. One of the most interesting features of the radial polarization is the formation of a large non-propagating longitudinal component of optical electric field near the beam axis. Conversely, the azimuthal polarization generates a strong magnetic field near the optical axis. Recently, Zhan [14] has studied the properties of circularly polarized vortex beams and has found the proper combination of polarization and topological charge of phase singularity to achieve focusing properties similar to radial polarization. Besides polarization, other parameters such as the pupil amplitude and phase structure of the field play an important role to achieve a very narrow beam with a long depth at focus, high beam quality and high optical efficiency. To this purpose, many different optical beam profiles have been studied both theoretically and experimentally, such as Bessel-Gauss (BG), Hypergeometric (HyG), Hypergeometric-Gaussian (HyGG), fractional elegant Laguerre-Gauss (fr-eLG), Ince-Gaussian, Laplace-Gauss and Mathieu beams [15, 16, 17]. Among them, the radially polarized BG beams have been to date proved to provide the best results. Moreover, Wang et al. [2] have recently calculated that an even tighter and deeper focus spot - a "light needle" - even smaller than the standard diffraction limit, can be obtained from BG beams by adding a suitable binary phase mask to the high numerical aperture focusing system.

In this article, we present a new family of solutions to the paraxial wave equation carrying finite power and having better features than the BG beams under strong focusing. The modes studied here have a hypergeometric amplitude profile as other modes introduced previously (HyG [16] and HyGG [17] modes), but differ from those in some important respects. For this reason, we propose to name these new modes "hypergeometric-gauss modes of the second type" (HyGG-II). Actually, these modes can be also regarded as a limit subfamily of circular beam (CiB) introduced in [15], where however, their special features under focusing were not analyzed or discussed. We studied the properties of the HyGG-II modes at the focus of a large aperture lens. In this work, we prove that HyGG-II beams may provide better spot size, beam quality and depth of focus than BG beams.

2. Hypergeometric-Gaussian type-II modes

The scalar Helmholtz paraxial wave equation in the cylindrical coordinates is given by

$$\left(\partial_{\rho,\rho} + \frac{1}{\rho} \partial_{\rho} + \frac{1}{\rho^2} \partial_{\phi,\phi} + 4i\partial_{\zeta} \right) \psi(\rho, \phi; \zeta) = 0, \quad (1)$$

where $\rho = \frac{r}{w_0}$, ϕ , $\zeta = \frac{z}{z_R}$ are dimensionless cylindrical coordinates. Here w_0 is the beam waist, $z_R = \frac{\pi w_0^2}{\lambda}$ is the beam Rayleigh range and λ is the beam wavelength. A family of solutions of Eq. (1) is given by

$$|\text{HyGG-II}\rangle_{pm} \equiv u_{pm}(\rho, \phi; \zeta) = C_{pm} \left(\frac{1}{1+i\zeta} \right)^{p/2+|m|+1} \times \rho^{|m|} e^{-\frac{\rho^2}{1+i\zeta}} e^{im\phi} {}_1F_1 \left(-\frac{p}{2}, |m|+1; \frac{\rho^2}{1+i\zeta} \right), \quad (2)$$

where m is an integer, p is a real number, $\Gamma(x)$ is the Gamma function, ${}_1F_1(a, b; x)$ is the confluent hypergeometric function and C_{pm} is the normalization factor given by $C_{pm} = \sqrt{\frac{2^{p+|m|+1}}{\pi \Gamma(p+|m|+1)} \frac{\Gamma(1+|m|+\frac{p}{2})}{\Gamma(|m|+1)}}$. This solution can be obtained as a limit case of Eq. (6) of [15] by setting $\gamma = -i(p+m+1)$, $q_0 = -iz_R$, and $\tilde{q}_0 \rightarrow \infty$. We see that C_{pm} stays finite as long as p is so that $p \geq -|m|$, which ensures that the power carried by HyGG-II beams is finite. Finally, the factor $\exp(im\phi)$ in Eq. (2) ensures that HyGG-II beams are eigenmodes of the photon orbital angular momentum. It can be shown that the HyGG-II modes, like the HyGG modes [17] (but unlike the HyG modes [16]), form a non-orthogonal set, i.e. $\langle \text{HyGG-II} \rangle_{p'm'} | \text{HyGG-II} \rangle_{pm} = \delta_{mm'} \frac{\Gamma(p/2+p'/2+|m|+1)}{\sqrt{[\Gamma(p'+|m|+1)\Gamma(p+|m|+1)]}}$. Moreover, the HyGG-II modes, unlike the HyGG and HyG ones, have no singularity at $\zeta = 0$. A very interesting property of

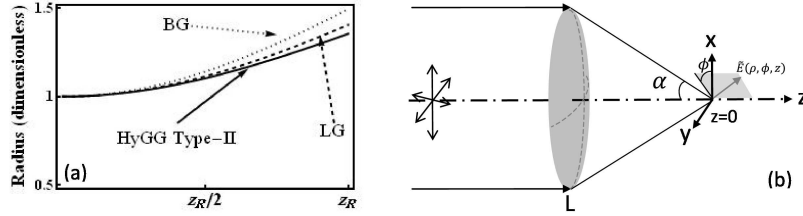


Fig. 1. (a) Variation of maximum intensity radius during the propagation for $\text{LG}_{0,1}$, BG_1 , $\text{HyGG-II}_{-1,1}$. (b) Scheme of the focusing system.

HyGG-II modes is that they suffer very low diffraction. In fact, the divergence angle at waist of the HyGG-II modes is smaller than of the BG and LG modes. Fig. 1(a) compares the variation of the maximum intensity radius of HyGG-II, BG and LG beams while they propagate along the z -axis. We see that HyGG-II has a slope 12.5% lower than LG beam and 28% lower than BG beam, where we define slope = $\frac{w(z_R)-w_0}{z_R}$. The HyGG-II modes may be generated from a plane-wave by the following unbounded transmittance function at $\zeta = 0$

$$u_{pm}(\rho, \phi, 0) = e^{-\rho^2+im\phi} \rho^{|m|} {}_1F_1 \left(-\frac{p}{2}, |m|+1; \rho^2 \right). \quad (3)$$

The asymptotic behavior of HyGG-II at large ρ is given by

$$u_{pm}(\rho, \phi, 0) \propto e^{-\frac{\rho^2}{1+i\zeta}} \rho^{p+|m|} + \frac{\rho^{-(p+|m|+2)}}{\Gamma(-\frac{p}{2})}. \quad (4)$$

Therefore, there are two asymptotic behaviors for the intensity $I_{p,m} = |u_{p,m}|^2$ depending on the radial number p ;

1. In the general case, $I_{p,m} \propto \rho^{-2(p+|m|+2)}$, i. e. a power law decay.

2. For nonnegative even integer number p , $I_{p,m} \propto \rho^{2(p+|m|)} e^{-\frac{2\rho^2}{1+\zeta^2}}$, i. e. a gaussian decay.

Because all zeros of the hypergeometric function are on the real axis, the intensity of the HyGG-II modes never vanishes in the transverse plane for $\zeta > 0$, except at $\rho = 0$ where the vortex singularity is located when $m \neq 0$. Finally, we will discuss briefly some possible subfamilies of the HyGG-II modes.

a) $p = |m| = 0$, in this case the mode is the gaussian TEM₀₀ beam.

b) $p = -|m|$ a negative integer number, the HyGG-II can be expanded as a superposition of two modified-Bessel beams;

$$u_{-|m|,m}(\rho, \phi; \zeta) = \frac{1}{\sqrt{2}} \left(\frac{1}{1+i\zeta} \right)^{3/2} e^{im\phi} \rho e^{-\frac{\rho^2}{2(1+i\zeta)}} \times \left[I_{\frac{|m|-1}{2}} \left(\frac{\rho^2}{2(1+i\zeta)} \right) - I_{\frac{|m|+1}{2}} \left(\frac{\rho^2}{2(1+i\zeta)} \right) \right] \quad (5)$$

where $I_n(x)$ is the modified Bessel function of integer order n . We call this sub-family “modified Bessel Gauss modes of type-II” (MBG-II), for distinguishing them from those introduced in [17].

c) For $p \geq 0$ even integer number, one can easily show that

$$u_{2n,m}(\rho, \phi; \zeta) = \sqrt{\frac{2^{2n+|m|+1}}{\pi\Gamma(2n+|m|+1)}} \Gamma(n+1) \left(\frac{1}{1+i\zeta} \right)^{n+|m|+1} \times e^{-\frac{\rho^2}{1+i\zeta}} \rho^{|m|} e^{im\phi} L_n^{|m|} \left(\frac{\rho^2}{1+i\zeta} \right). \quad (6)$$

which are the well-known “elegant Laguerre-Gauss” (eLG) beams [15].

d) For $p > 0$ odd integer number, the HyGG-II modes reduce to a polynomial superposition of the modified Bessel functions $I_0(x)$ and $I_1(x)$. We will call this sub-family “modified-polynomial Bessel-Gauss” (MPBG) beams.

3. Hypergeometric-Gaussian-II modes under strong focusing

In this section, we study some properties of HyGG-II in the focal region of a high numerical aperture lens. Let us consider an aplanatic high-numerical-aperture focusing lens system (see Fig. 1(b)). The origin $z = 0$ is located at the lens focal point, f , NA, $\alpha = \arcsin(\frac{\text{NA}}{n})$, and $n = 1$ are the focal length, the numerical aperture, the semi-aperture angle, and the vacuum refractive index, respectively. Using the vectorial Debye diffraction integral, Richard and Wolf [11] have shown that the electric field at the point $\tilde{r} = (\rho, \phi, z)$, in a region close to the focal point in the cylindrical coordinates is given by

$$\tilde{E}(\tilde{r}) = -\frac{i}{\lambda} \iint_{\Omega} \tilde{a}(\theta, \varphi) e^{2\pi i(z \cos \theta + \rho \sin \theta \cos(\varphi - \phi))} d\Omega, \quad (7)$$

where $\tilde{a}(\theta, \varphi)$ is determined by the field distribution in the object space at the pupil and Ω is the solid angle. In Eq. (7), ρ and z are dimensionless, their scale length being the λ . Youngworth and Brown [12] have calculated this integral for radially and azimuthally polarized beams. Their

calculation showed that the radial polarization is much more effective than the azimuthal and linear ones for obtaining a tight focusing. Therefore, we restrict our attention only to radially polarized beams. The electric field of a radially polarized beam in the focal region is given by

$$\begin{aligned} E_\rho(\tilde{r}) &= \frac{f}{\lambda} \int_0^\alpha \sqrt{\cos \theta} \sin(2\theta) l(\theta) J_1(2\pi\rho \sin \theta) e^{i(2\pi z \cos \theta)} d\theta \\ E_z(\tilde{r}) &= \frac{2if}{\lambda} \int_0^\alpha \sqrt{\cos \theta} \sin^2 \theta l(\theta) J_0(2\pi\rho \sin \theta) e^{i(2\pi z \cos \theta)} d\theta, \end{aligned} \quad (8)$$

where $J_0(x)$ and $J_1(x)$ are Bessel's functions, and $l(\theta)$ is the amplitude distribution of the pupil apodization function. We consider an amplitude-only apodization function given by the

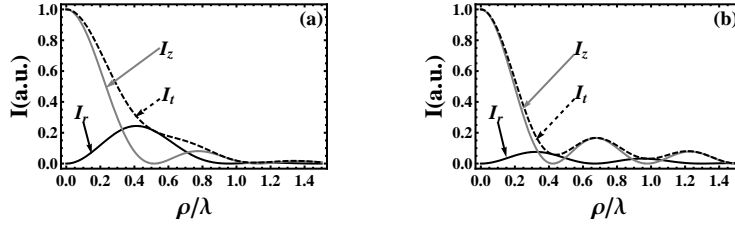


Fig. 2. Intensity profile of the longitudinal and radial field components at the focal point of a high numerical aperture lens (a) and a system of high numerical aperture lens and binary phase mask (b). The black, gray and dashed lines are radial, longitudinal and total intensity, respectively.

HyGG-II_{-1,1} profile calculated from Eq. (3) with the singular phase factor omitted. We choose this profile because it exhibits minimum diffraction. Explicitly, $l(\theta)$ is given by

$$l(\theta) = e^{-\beta^2 \left(\frac{\sin \theta}{\sin \alpha}\right)^2} \left(\beta \frac{\sin \theta}{\sin \alpha} \right) {}_1F_1 \left(\frac{1}{2}, 2; \beta^2 \left(\frac{\sin \theta}{\sin \alpha} \right)^2 \right), \quad (9)$$

where β is the ratio between the pupil radius and the beam waist. One can solve the integral in Eq. (9) numerically and plot the intensities near the focus for any values of the numerical aperture. The numerical integrations were performed using global adaptive algorithms, which recursively subdivide the integration region as needed. In our calculations we considered $\beta = 1$ and $\text{NA} = 0.95$ corresponding to $\alpha = 71.8^\circ$. We compared our results with the well-known apodization function of the BG₁ beam. Fig. 2(a) shows the intensity profile of the radial and longitudinal components of the optical field at focus. It is evident that the intensity of the longitudinal component is higher than the radial component. The beam quality is characterized by [2]

$$\eta = \frac{\int_0^{r_0} |E_z(r, 0)|^2 r dr}{\int_0^{r_0} |E_\rho(r, 0)|^2 r dr + \int_0^{r_0} |E_z(r, 0)|^2 r dr} \quad (10)$$

where r_0 is the first zero of the radial field component. For the HyGG-II_{-1,1} profile we found $\eta = 52.5\%$ instead of 44.7% for the BG₁ profile in the same conditions. The hypergeometric apodization function increases the beam quality by 17%. Furthermore, the HyGG-II_{-1,1} beam size (full width at half maximum, FWHM) is as small as 0.60λ which is 13% less than the beam size of the BG₁ mode (although it is still larger than diffraction limit). Also, its depth focus is about $\sim 1.5\lambda$ which is 1.4% larger than the depth focus of the BG₁ mode. Finally, we

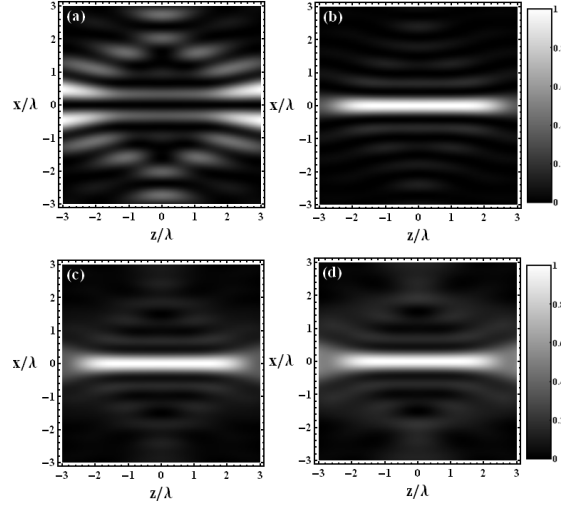


Fig. 3. Density plots of intensity distribution for (a) radial, (b) longitudinal components. (c) and (d) show the total intensity distribution for the HyGG-II_{-1,1} and the BG₁ beams, respectively.

calculated the optical electric field near the focal point when a binary phase mask is inserted just in front of the high numerical aperture system, as in [2]. Our binary phase mask is made of five concentric belts in which the phase of each belt changes by π with respect to neighbor belts [18, 2]. Compared with the mask used in [2] for the BG₁ modes, we introduced some small modifications, i.e., $\theta_1 = 4.46^\circ$, $\theta_2 = 23.64^\circ$, $\theta_3 = 36.53^\circ$, $\theta_4 = 49.03^\circ$, where θ_i are related to the inner radius of each belts, $r_i = \sin \theta_i / \text{NA}$. The intensity profiles of the radial and longitudinal components of the field in the presence of this phase mask are shown in Fig. 2(b). The total field FWHM is 0.426λ , leading to a spot size of $0.142\lambda^2$. These values are 1.6% and 3.2% smaller than the in BG₁ case [2]. Furthermore, the phase mask increases the beam quality to 81.76%, which is improved by 1.7% with respect to the BG₁ profile. Fig. 3 shows the intensity distribution for the radial Fig. 3(a), longitudinal Fig. 3(b) and total field Fig. 3(c) of the HyGG-II_{-1,1} profile. For the sake of comparison, the total field of the BG₁ profile is shown in Fig. 3(d). It is clear that the depth of focus of the hypergeometric profile is longer than the Bessel-Gauss case and it is about 4.5λ .

It is also worth investigating the field distribution obtained at the focus when using vector vortex beams [14] having the HyGG-II profile of Eq. (3) with the singular phase retained, but we postponed this problem to the near future.

4. Conclusion

In conclusion, we studied a novel family of paraxial beams having singular profile. All modes of this family are eigenmodes of the orbital angular momentum of light and are an overcomplete nonorthogonal set of modes. Moreover, the modes of this family exhibit a diffraction divergence at waist which is the smallest among all other known modes carrying a finite power. As a consequence, we found that these beams, when radially polarized, can be focused into a tighter and longer region, compared with other known modes. A small improvement compared with other modes is obtained also when the focusing is pushed below the diffraction limit by adding a suitable phase mask.